Isospin mixing in ^{24}Mg

C. D. Hoyle,* E. G. Adelberger, J. S. Blair,† K. A. Snover,
H. E. Swanson, and R. D. Von Lintig‡
Nuclear Physics Laboratory, University of Washington, Seattle, Washington 98195
(Received 8 November 1982)

We have used the β-γ circular polarization correlation technique to measure the isospin-forbidden Fermi matrix element for the β^+ decay of ^{24}Al to the 4^+ $T=1$ state in ^{24}Mg at $E_x=8.439$ MeV. The ^{24}Al activity was produced by bombarding a natural Mg target with 18 MeV protons. The β-γ circular polarization correlation was measured using a novel apparatus which featured good energy resolution in both the γ and β arms. The circular polarization sensitive γ-ray detector utilized a transmission-mode Compton polarimeter and a 12.7 cm $\times$15.2 cm NaI detector. The β detector was a telescope with a 700 μm surface barrier detector and a 5.1 cm $\times$12.7 cm plastic scintillator. The β-γ circular polarization asymmetry $\tilde{A}$ [defined by $W(\theta,\tau)=1+\tau v/c\tilde{A}\cos\theta$ where τ is the photon helicity] was found to be $\tilde{A}=-0.145\pm0.030$. After applying a correction for feeding of the 8.439 MeV state from the analog state this value of $\tilde{A}$ corresponds to a charge dependent matrix element between the 9.5 MeV 4^+ $T=1$ and 8.4 MeV $T=0$ levels of $|\langle 4^+;0|H_{CD}|4^+;1\rangle|=106\pm40$ keV which is the largest matrix element of H_{CD} ever observed in β decay. For comparison the charge dependent matrix element between the 9.5 MeV state and the 4.1 MeV 4^+ state, previously measured in ^{24}Na decays is only 5.4 ± 2.2 keV. Our exceptionally large value occurs because the 9.5 MeV $T=1$ and 8.4 MeV $T=0$ states have very similar space and spin wave functions. This matrix element is consistent with predictions which ascribe the entire effect to Coulomb forces.

[RADIOACTIVITY ^{24}Al [from ^{24}Mg(p,n)]; measured $\beta\gamma$ CP correlations; developed new apparatus; measured isospin forbidden Fermi matrix element. Deduced isospin mixing matrix element.]

I. INTRODUCTION

The Fermi β decay matrix element provides the only rigorous, model-independent measure of the isospin purity of nuclear states. The observation of a nonzero Fermi matrix element between states of nominally different isospin directly yields the isospin nonconserving matrix element connecting the two states. There now exists quite a body of data[1–4] on the sizes of isospin-mixing matrix elements determined in this completely unambiguous fashion. The results, for nuclei with $A\leq80$, are shown in Fig. 1. The deduced matrix elements are typically very small, say ~10 keV, the two largest known values[1] being 56 ± 12 and 41.7 ± 1.1 keV in ^{57}Ni and ^{64}Ga decays, respectively.

Isospin admixtures can also be probed by less rigorous, but far more convenient, techniques. Two methods have found particularly wide application: measurements of isospin-retarded electromagnetic transitions, and the study of departures from the Adair rules for nuclear reactions related by the isospin symmetry. In several cases these electromagnetic (EM) and strong probes of isospin mixing have yielded very large values for $|\langle H_{CD}\rangle|$. Notable examples are the ~140 keV matrix element[5,6] connecting the 16.6 and 16.9 MeV 2^+ states in ^{8}Be, the 140 ± 35 keV matrix element[7,8] connecting the 12.7 and 15.1 MeV states of ^{12}C, and the $\geq155\pm30$ keV matrix element[9] connecting the 12.53 and 12.97 MeV states of ^{16}O. However, the EM and strong probes of isospin mixing are model dependent. Although measurements of isospin mixing by electromagnetic transitions use a well-understood interaction, the extraction of $\langle|H_{CD}|\rangle$ requires a shell model calculation of the EM matrix element for the isospin retarded transition. Strong interaction probes of isospin mixing rely, in addition, on a reaction model to distinguish "residual" effects (Q-value differences, Coulomb interactions in the entrance and exit channels, etc.) from the "interesting" effects due to isospin impurities.

The clear discrepancy between the large values of $|\langle|H_{CD}|\rangle|$ inferred from the model-dependent

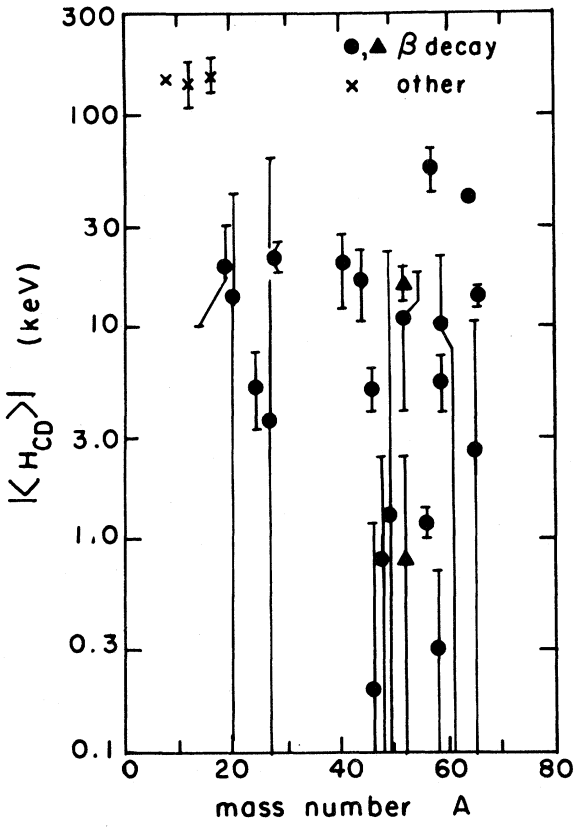

FIG. 1. Values for the off-diagonal isospin mixing matrix elements $|\langle|H_{CD}|\rangle|$. Results inferred from isospin-forbidden Fermi matrix elements were taken from Refs. 1, 3, and 4 and are denoted by solid dots and triangles. Results inferred by less rigorous means (see Refs. 5–7) are denoted by crosses. The measurement described in this paper is not shown in the figure.

EM and strong probes and the smaller values of $|\langle|H_{CD}|\rangle|$ determined by the model-independent weak probe raises interesting questions. Is this difference due to an invalid analysis of the model-dependent probes or does it rather reflect some physical difference between the systems studied by the model-independent and the model-dependent probes? What could these physical differences be?

The large values for $|\langle|H_{CD}|\rangle|$ determined by EM and strong probes all occur in self-conjugate nuclei. However, β decay experiments[1] have yielded a value of 14^{+29}_{-14} keV for the charge dependent matrix element connecting the 1.63 MeV 2^+ $T=0$ and 10.27 MeV 2^+ $T=1$ levels of ^{20}Ne and a value of 5.4±2.2 keV for that connecting the 4.12 MeV 4^+ $T=0$ and 9.52 MeV 4^+ $T=1$ levels of ^{24}Mg, so the large matrix elements cannot be explained as a consequence of T_3 being zero.

A more likely possibility for the striking difference in the sizes of $|\langle H_{CD}|\rangle|$ determined by the two classes of probe lies in the structures of the states involved. The Coulomb force, being a long-range, spin-independent interaction, has large off-diagonal matrix elements when the two states have wave functions with very similar space and spin structure. Those cases in which large matrix elements are observed do, in fact, all involve a pair of states with very similar space and spin wave functions. On the other hand, without exception, previous β decay experiments detected the mixing between the $T_>$ analog state and the *lowest*-lying $T_<$ state having the same J^π as the analog state. In general these low-lying states will not have a wave function which is related in a simple way to that of the analog state and therefore are connected to the analog level with small charge dependent matrix elements. This could explain the discrepancy between the β decay and the other probes of isospin mixing.

In this paper we report the first measurement, using β decay methods, of a charge-dependent matrix element for a case in which one expects[10] to find a very large value—namely two states in a self-conjugate nucleus which have very similar space and spin structure. In particular we measure (see Fig. 2) the Fermi matrix element for the decay of ^{24}Al to the 4^+ $T=0$ level in ^{24}Mg at $E_x=8439$ keV and observe the largest value of $|\langle|H_{CD}|\rangle|$ ever detected in β decay experiments, 106±40 keV. The previously observed Fermi component for the decay of ^{24}Na to the 4^+ $T=0$ level at $E_x=4123$ keV corre-

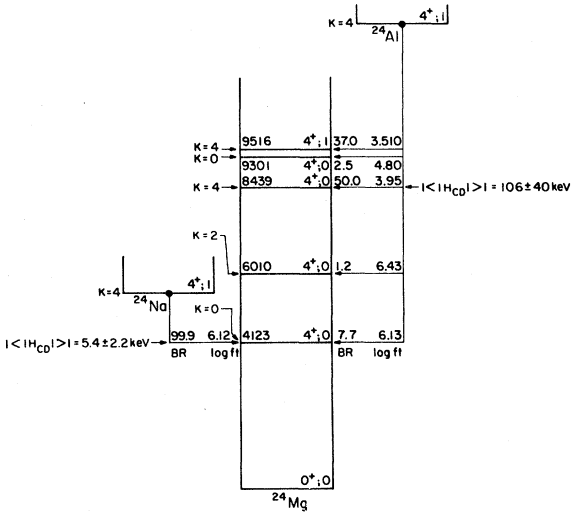

FIG. 2. Beta decays of the 4^+ $T=1$ states in $A=24$. The ^{24}Al branching ratios and logft values along with the K assignments are from Ref. 11. The values of $|\langle|H_{CD}|\rangle|$ from ^{24}Na and ^{24}Al decays are taken from Ref. 1 and this work, respectively.

sponds[1] to a matrix element of only 5.4±2.2 keV. Our large value, and the small one for the 4123 keV transition, are explained by quite simple considerations. In the Nilsson model the ^{24}Al ground state and ^{24}Mg (8439) both have $K=4$ while ^{24}Mg (4123) has $K=0$ (see Ref. 11) so that the analog-8439 keV mixing is K allowed while the analog-4123 keV mixing is K forbidden. Our result thus indirectly supports the large values of $|\langle|H_{CD}|\rangle|$ obtained in other nuclei by less rigorous means.

II. THEORY OF MIXED FERMI-GAMOW-TELLER TRANSITIONS

Consider a general β-γ transition with a nuclear spin sequence

$$J\xrightarrow{\beta}J'\xrightarrow{\gamma}J'' .$$

The nuclear matrix element for the β transition can be expressed as

$$\langle J'||G_V M_V||J\rangle+\langle J'||G_A M_A||J\rangle$$

where V and A refer to the vector and axial-vector weak hadronic currents. We define the Fermi to Gamow-Teller (GT) mixing ratio as

$$y\equiv\frac{\langle J'||G_V M_V||J\rangle}{\langle J'||G_A M_A||J\rangle}$$

and restrict ourselves to the allowed approximation. If the nuclear states are isospin eigenstates $y=0$ unless the initial and final states belong to the same isospin multiplet in which case

$$\langle J'||M_V||J\rangle=\sqrt{2T} .$$

If we consider a $T\to T'=T-1$ transition and include, to lowest order, the effects of isospin impurities, $M_F=\alpha\sqrt{2T}$ where α is the amplitude of the analog of the initial state in the final state. The β decay half-life is given by

$$ft=\frac{K}{|\langle J'||G_V M_V||J\rangle|^2+|\langle J'||G_A M_A||J\rangle|^2} ,$$

where K may be evaluated from the superallowed 0^+, $T=1\to0^+$, $T=1$ Fermi transitions for which ft is observed to be $ft_0=3088.6\pm2.1$ sec and we assume

$$\langle J'||M_V||J\rangle=\sqrt{2} .$$

Since the V and A matrix elements do not interfere in the expression for ft it is clear that the ft value of a predominantly GT transition will not in general provide an unambiguous means of measuring a small isospin forbidden Fermi matrix element. Small values of α are best measured in experiments which detect pseudoscalars and thus probe the V,A interference. This is conventionally done by detecting the β-γ circular polarization (CP) correlation $\hat{k}_e\cdot\hat{k}_\gamma\hat{k}_\gamma\cdot\hat{\sigma}_\gamma$, where the $\hat{k}$'s are propagation vectors and $\hat{\sigma}_\gamma$ is the photon spin.

The β-γ angular correlation for a CP-sensitive γ-ray detector will be

$$w(\theta,\tau)=1+\tau(v/c)\tilde{A}\cos\theta ,$$

where $\cos\theta=\hat{k}_\beta\cdot\hat{k}_\gamma$, v is the β velocity, and $\tau=+1$ (-1) for right (left) handed circularly polarized γ rays. Let the $J'\to J''$ γ transition proceed via multipole order λ with a possible admixture of multipole order $\lambda+1$. We define the multipole mixing ratio

$$\delta=\frac{\langle J''||\mathcal{O}(L+1)||J'\rangle}{\langle J''||\mathcal{O}(L)||J'\rangle} .$$

The asymmetry coefficient $\tilde{A}$ is given[12] by

$$\tilde{A}=\frac{\sqrt{3}}{6(1+y^2)}\left\{\mp\frac{J'(J'+1)-J(J+1)+2}{[J'(J'+1)]^{1/2}}+4y\right\}\left\{\frac{F_1(\lambda,\lambda,J'',J')+2\delta F_1(\lambda,\lambda+1,J'',J')+\delta^2F_1(\lambda+1,\lambda+1,J'',J')}{1+\delta^2}\right\},$$

where the F_1 coefficients are familiar from γ-ray angular correlation theory, and the upper (lower) sign refers to β^- (β^+) decay. The physical significance of this expression is made clear by rewriting it as $\tilde{A}=A_1(\beta)A_1(\gamma)$, where

$$A_1(\beta)=\frac{\sqrt{3}}{6(1+y^2)}\left\{\mp\frac{J'(J'+1)-J(J+1)+2}{\sqrt{J'(J'+1)}}+4y\right\}$$

is the vector polarization of the state J' produced in the β decay and $A_1(\gamma)$ gives the amount of CP carried off by the γ-ray deexciting a vector polarized state (see Ref. 13).

Later we shall need the β-γ CP correlation for a

$$J\xrightarrow{\beta}J'\xrightarrow{\gamma_1}J''\xrightarrow{\gamma_2}J'''$$

transition in the case where the first γ radiation, γ_1, is unobserved and we instead detect the β-γ_2 CP correlation. Then the expression for $\tilde{A}$ involves a deorientation coefficient[13] U_1 (γ_1) to account for the unobserved γ_1 transition

$$\tilde{A}=A_1(\beta)U_1(\gamma_1)A_1(\gamma_2) .$$

In the case of a $J;T \rightarrow J;T-1$ transition the allowed Fermi matrix element vanishes if the states have good isospin. Charge dependent forces will induce a small Fermi matrix element and, as discussed below, $\langle J;T-1 \mid H_{CD} \mid J;T \rangle$ can be inferred from a measurement of y.

III. APPARATUS

The β activity was produced in the standard fashion by bombarding thin targets mounted in balsa wood "rabbits" which were shuttled between the bombardment station and a well shielded counting area. The rabbit was propelled to the counting area by a blast of air and pulled back into the bombardment station by a partial vacuum.

We measured $\tilde{A}$ by observing coincidences of β's emitted at $\sim 180°$ to γ rays detected in a CP sensitive detector. The analyzing efficiency η of the CP sensitive detector, defined by

$$\eta = (f_R - f_L)/(f_R + f_L) ,$$

where f_R and f_L are the fractions of incident right (left) handed γ rays which are counted by the γ detector, can easily be reversed. We observed an equal number of β decays with each sign of η and obtained $\tilde{A}$ from the relation

$$\tilde{A} = \frac{N_+ - N_-}{N_+ + N_-} \frac{1}{\eta \langle v/c \rangle \langle \cos(\theta) \rangle} ,$$

where N_+ (N_-) is the number of β,γ coincidences when the circular polarimeter preferentially accepts right (left) handed γ rays. The quantities $\langle v/c \rangle$ and $\langle \cos(\theta) \rangle$ are averaged over the range of accepted β energies and detector solid angles, respectively.

Since we were interested in detecting the β-γ CP correlation of a transition to a highly excited state of the daughter nucleus we had to develop an instrument which differed significantly from previous apparatus. The most important requirement was good energy resolution in both the β- and the γ-ray arms. The β-γ CP correlation apparatus is shown schematically in Fig. 3.

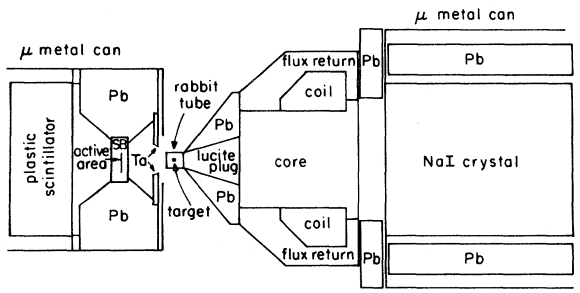

FIG. 3. Scale drawing of the β-γ CP correlation apparatus. The core of the circular polarimeter is constructed of 2V-Permendur while the flux return is Armco iron. The unit labeled SB is a totally depleted surface barrier detector. The rabbit travels in and out of the plane of the figure.

The polarimeter was one of four constructed at Chalk River by McDonald for a measurement of the parity violating CP of the 2.8 MeV γ ray in ^{21}Ne.[14] It was well suited for the present experiment because of its large solid angle. The current which excited the polarimeter magnets was provided by a constant-current supply which fed a full-wave transistor bridge. The bridge circuit allowed a digital signal to reverse the current with essentially no change in its magnitude. The polarimeter was flipped after each cycle of the rabbit. For this experiment two changes were made in the polarimeter. The heavy metal cube which, in the ^{21}Ne experiment, collimated the γ rays into the four polarimeters was replaced with a conical Pb collimator whose aperture was filled with a Lucite plug, and the excitation current was lowered from 4.5 to 2.5 A. The Lucite plug stopped the high energy β's with minimum bremsstrahlung. The reduced excitation current was selected to minimize the stray B fields from the polarimeter magnet. The current was chosen by measuring the magnetization of the polarimeter core as a function of excitation current. The excitation current was flipped once each second and the magnetization detected by electronically integrating the output of a sense coil wound around the polarimeter core. The reduction of the excitation current from 4.5 to 2.5 A significantly reduced the stray fields at the cost of diminishing the integrated sense coil output by 1.7% and increasing the flipping time from 340 to 575 msec. Since the polarimeter was flipped just after the rabbit was retracted into its bombardment station the increased flipping time was no disadvantage. The NaI detector was inside a magnetic shield. When the polarimeter magnetization was flipped the B at the phototube changed by only 0.05 G. The measured gains for the two polarimeter states differed by a factor of only 10^{-4}.

The β detector was a ΔE-E telescope. It consisted of a 300 mm^2 ORTEC surface barrier detector with a thickness of 700 μm and a 12.5 cm diam by 5.1 cm thick plastic scintillator coupled to an RCA 4522 photomultipler. Electrons leaving the rabbit target were roughly defined by a Ta collimator. The ΔE detector was mounted in a Pb shield which reduced the probability for $\beta\gamma\gamma$ coincidences in which a β and one gamma ray were summed in the plastic scintillator. The entire β detector system was enclosed in a cylindrical magnetic shield which attenuated the stray field from the γ-ray circular polarimeter. Electrons entered the detector through a 3.75 cm diam hole in the shield. This shield reduced

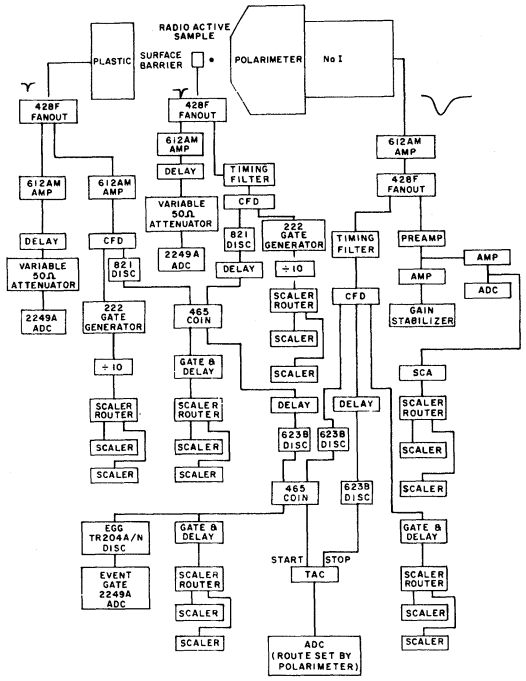

FIG. 4. Schematic diagram of the signal processing electronics. The numbers on the various units refer to manufacturer's model numbers. Unless otherwise noted the units with model numbers were manufactured by Lecroy or ORTEC.

systematic errors from two sources—deflection of the β particles and gain shifts in the scintillation detector. When the polarimeter magnetization was reversed the axial $\vec{B}$ field changed by 35 G at the counting position of the target, by 18.5 G at the entrance hole in the magnetic shield, by 0.78 G at the surface barrier detector, and by 0.06 G at the photomultiplier. We tested the effectiveness of the shield by observing the changes in the rate of ΔE-E coincidences when the polarimeter was reversed. In a perfect detector there should be no change since we did not require coincidences with the γ ray. Without the magnetic shield in place the observed ΔE-E coincidence rate changed by ~ 1–$2\,\%$ when the polarimeter was reversed. With the shield in place this change was reduced to $\sim 0.05\%$. The γ-ray rejection efficiency of the β detector was measured using an encapsulated ^{22}Na source from which β^+'s could not escape. The rate of surface barrier-plastic scintillator coincidences was compared to the singles rate in the plastic scintillator. The ratio of the two rates was $(1.5\pm 0.1)\times 10^{-3}$, which was adequate for our needs.

The signal-processing electronics for our apparatus is shown schematically in Fig. 4. For each β-γ coincidence five signals are recorded—the pulse heights in the NaI, surface-barrier and plastic scintillator detectors, the output of a time-to-amplitude converter (TAC) which measured the β-γ time difference, and the integrated sense coil output which recorded the instantaneous value of the magnetization in the polarimeter core. The TAC spectrum was routed two ways according to the state of the signal which controlled the polarimeter magnetization. This gave us an independent check that the magnetization was reversing properly. Event-mode data were written on magnetic tape by a PDP-11/60 computer which ran the MULTI program.

The electronics were required to handle very high singles rates. For the $^{24}\mathrm{Al}\rightarrow{}^{24}\mathrm{Mg}(4^+;8.4$ MeV$)\rightarrow{}^{24}\mathrm{Mg}(2^+;1.4$ MeV) decay sequence the expected value for the "true" fractional change in counting rate upon flipping the polarimeter is $\sim 4\times 10^{-3}$. To obtain a statistical error of 1×10^{-3} in this quantity, approximately 10^6 true coincidences are required. Combining this estimate with the attenuation of γ rays by the polarimeter, the branching ratios of the $^{24}\mathrm{Al}\rightarrow{}^{24}\mathrm{Mg}(4^+)\rightarrow{}^{24}\mathrm{Mg}(2^+)$ decay sequence, and the photopeak efficiency of the NaI detector, we find that the instantaneous singles rates in the plastic scintillator and surface barrier detectors must be $\gtrsim 1$ MHz to obtain a statistical error of $\sim 1\times 10^{-3}$ in ~ 10 d of running time. The singles rate in the NaI detector will of course be much lower (~ 30 kHz at a discriminator threshold of ~ 1 MeV).

Because of the high singles rates in the β telescope we used fast negative signals from the surface barrier and plastic scintillator for the linear as well as the timing functions. These fast negative pulses were digitized by fast-gated integrating ADC's (LECROY 2249A). The lower rate TAC, NaI, and sense-coil signals were digitized by conventional ADC's. The discriminators were constant-fraction units designed at Berkeley. All coincidence timing was done using overlap units with the pulse-widths adjusted so that the threefold (NaI $\otimes$ surface barrier $\otimes$ plastic scintillator) coincidence time was determined by the plastic scintillator. This allowed us to start the TAC on the threefold coincidence signal and stop it on the NaI signal. Compared to the conventional scheme in which the TAC is started on a singles pulse, our scheme gave much smaller dead time losses in the TAC.

IV. CALIBRATION OF THE CIRCULAR POLARIMETER EFFICIENCY

The analyzing power, η, of a circular polarimeter may be defined by

$$\eta\equiv\frac{N_R^+-N_R^-}{N_R^++N_R^-}\ ,$$

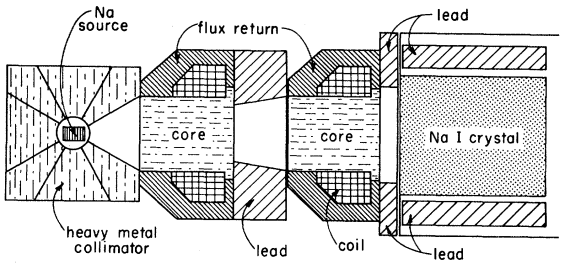

FIG. 5. Scale drawing of the setup used to calibrate the circular polarimeter efficiency using the 2.75 MeV ^{24}Na γ ray.

where N_R^+ and N_R^- are the number of right-handed γ rays transmitted when the polarimeter $\vec{B}$ field is antiparallel and parallel to $\hat{k}_\gamma$, respectively. We measured the square of η for 2.754 MeV γ rays using $\sim$40 mCi ^{24}Na sources prepared by irradiating sodium fluoride powder at the University of Washington reactor.

The efficiency measurement was performed using two identical polarimeters as shown schematically in Fig. 5. The polarimeter $P1$, closest to the ^{24}Na source, had a steady magnetic field and partially polarized the ^{24}Na γ rays. This polarization was analyzed by the second polarimeter $P2$, whose magnetic field was reversed every 3.0 sec. In order to reduce the time required to reverse $\vec{B}$ the current in the polarimeters was kept at 4.5 A, the value used in the ^{21}Ne parity mixing experiment. Counting was disabled for 420 msec after each B reversal to avoid switching transients. Transmitted γ rays were counted in the same NaI detector used in the β-γ CP correlation experiment. The high voltage of the NaI detector was controlled by a gain stabilizer which fixed the position of the 2.75 MeV photopeak. NaI signals were fed into a fast pulse-height analyzer and routed into two regions of analyzer memory according to the direction of $\vec{B}$ in $P2$. Counting losses were monitored using a repetitive pulser which injected signals into the NaI preamp. The polarimeter magnetization was controlled by the pulser, being reversed after every 10^4 pulses. Since the total number of pulser events was known for each of the two routed NaI spectra we could correct for dead time and pileup effects.

TABLE I. Measurement of $|\eta|$ for 2.75 MeV gamma rays.

Configuration[a]	$(r-1)\times10^4$	$\|\eta\|\times10^2$
NN	24 ±2.4	
NR	23 ±3	
RN	26 ±2.4	
RR	20 ±2	
Sum	23.0±1.2	3.39±0.09

[a]RN, for example, refers to the configuration in which the polarity of $P1$ is reversed (R) and the leads to $P2$ are normal (N).

We obtained $|\eta|$ from the expression

$$\eta^2=(r-1)/(r+1)$$

where $r=N_p/N_a$ and N_p and N_a refer to the number of 2.75 MeV γ rays transmitted when the magnetic fields in the two polarimeters were parallel and antiparallel, respectively. Two small corrections

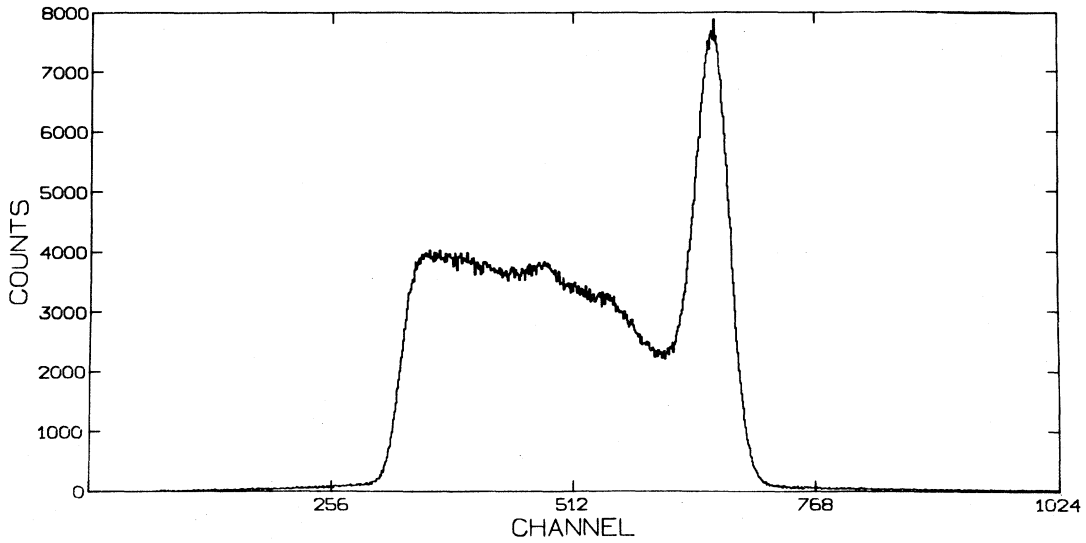

FIG. 6. Spectrum of γ rays from ^{28}Al decays. Although the continuum contains γ rays scattered by the polarimeter the photopeak consists almost entirely of γ rays which did not scatter in the polarimeter.

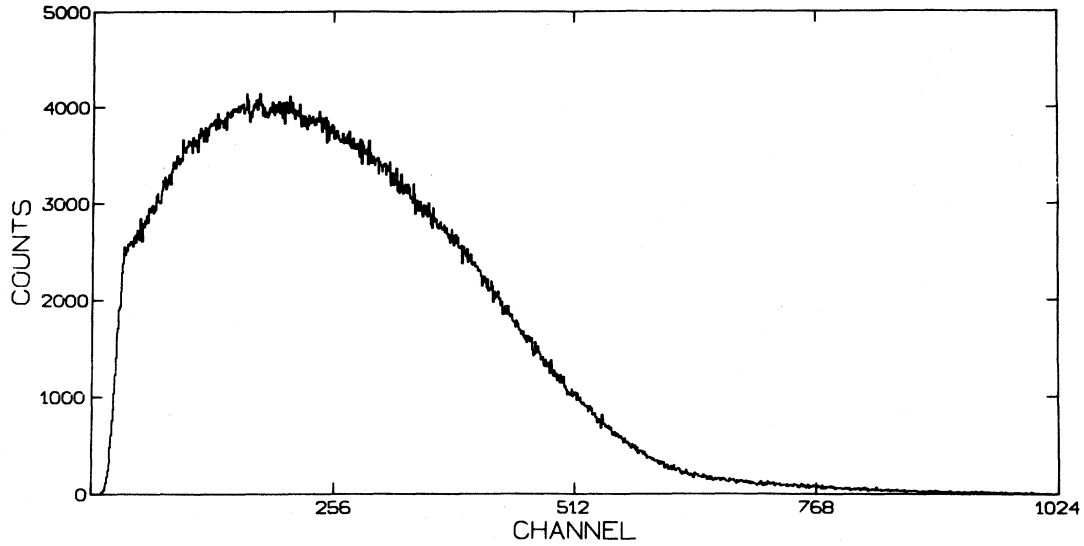

FIG. 7. Spectrum of pulse heights in the plastic scintillator from ^{28}Al decays.

were applied to r; the first to account for the decay of the ^{24}Na source and the second (typically a few parts in 10^4) to account for dead time and pileup differences as mentioned above. Comparable amounts of data were accumulated with both polarities of the field in $P1$ and with the current carrying leads to $P2$ in their normal and reversed configurations. By summing the results taken with all four of these configurations most of the potential systematic errors in our measurement are greatly diminished. The results from six ^{24}Na sources are shown in Table I.

The above data consisted of 16 runs. The 16 individual values of r have a standard deviation which is 1.09 times that expected from statistical errors alone, which indicates that nonstatistical fluctuations are not important. There is some evidence that the configurations with $P2$ reversed give somewhat smaller values of r than those with $P2$ normal, but it is hardly significant statistically.

We obtain the sign of η from theory since $\eta = k\sigma_1$, where k is a negative constant which depends on the polarimeter but not on E_γ, and σ_1 is the spin-dependent Compton cross section (defined, for example, in Ref. 15) which is a function of E_γ. We adopt the value

$$\eta(E_\gamma = 2.754 \text{ MeV}) = (3.39 \pm 0.09) \times 10^{-2} .$$

After k has been determined for the particular value of $E_\gamma = 2.754$ MeV it is straightforward to compute

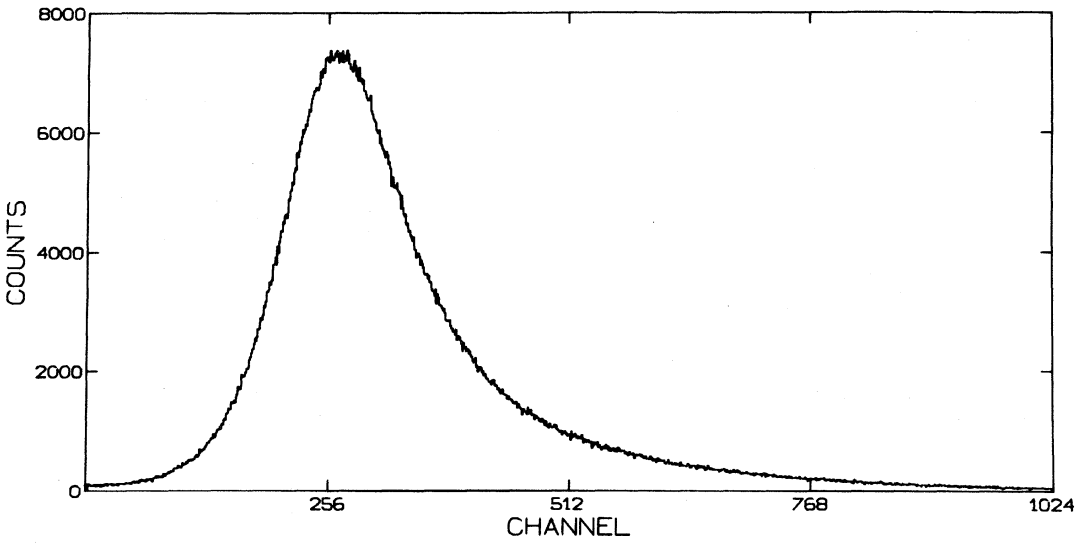

FIG. 8. Spectrum of pulse heights in the surface barrier detector from ^{28}Al decays.

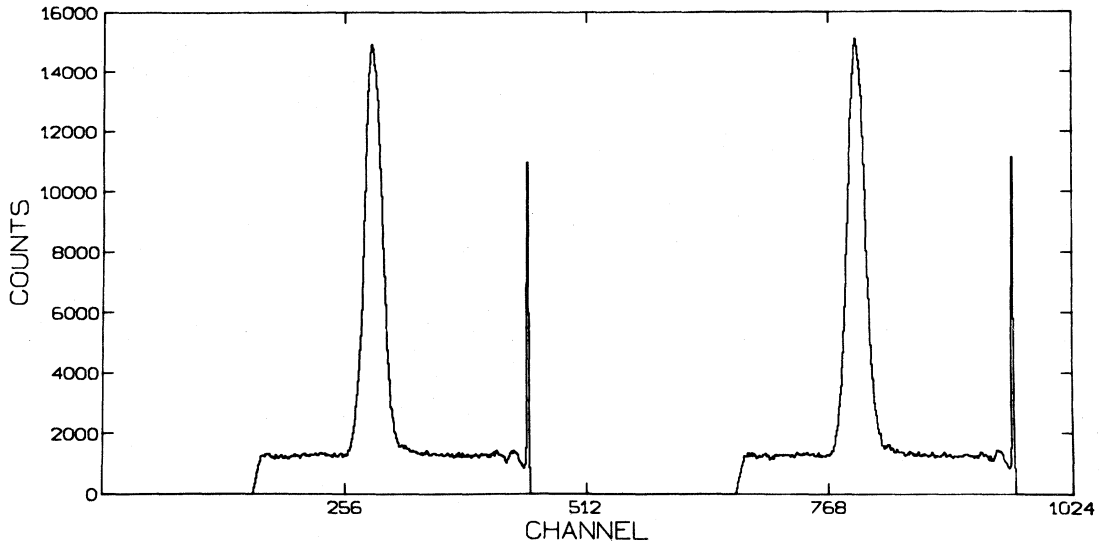

FIG. 9. TAC spectrum for ^{28}Al decays. One channel corresponds to 0.17 nsec.

η for any other value of E_γ using the known form of σ_1.

V. TEST OF THE APPARATUS USING KNOWN TRANSITIONS

In order to have confidence in our technique for detecting isospin mixing in ^{24}Mg we verified the performance of our apparatus and analysis by measuring the β-γ CP correlation of transitions for which $\tilde{A}$ could be predicted exactly. Of course, the "exactness" of the prediction relies upon the validity of the V-A theory and allowed approximation for the β decay process, but any uncertainties on these grounds are completely insignificant for our purpose.

A. The β^- decay of ^{28}Al

Our first test case was the β^- decay of ^{28}Al. This is a

$$J=3\rightarrow J'=2\rightarrow J''=0$$

spin sequence so that both y and δ are constrained to be zero by the allowed approximation and angular momentum conservation, respectively. In this case we expect $\tilde{A}=-\frac{1}{3}$. We chose ^{28}Al as a test case be-

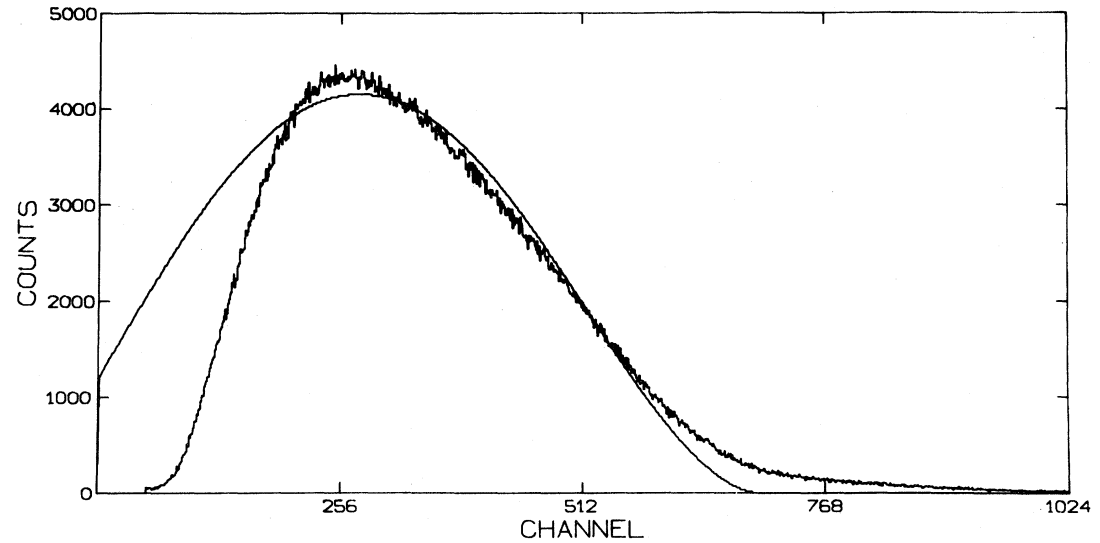

FIG. 10. Total β^- energy spectrum for ^{28}Al decays (see text). The solid curve is the expected shape for an ideal detector.

cause it has only one $\beta\gamma$ branch with a large value of $\tilde{A}$, and because it was convenient experimentally.

We produced the ^{28}Al activity by bombarding 25 μm Al foils with a 6 MeV deuteron beam. Although the ^{28}Al half-life is 2.24 min we used a 10 sec rabbit cycle (4.5 sec irradiation, 4.5 sec counting, and 0.5 sec for each transit). The ^{28}Al β^- decay has an end point of 2.86 MeV and produces a 1.78-MeV γ ray. Typical spectra for the NaI, plastic scintillator and surface barrier detectors, and the TAC are shown in Figs. 6–9. Energy calibrations of the three detector signals were performed using radioactive sources. The plastic scintillator calibration was done using the high energy edges of Compton electrons produced by a series of γ-ray sources while the surface barrier detector was calibrated using the conversion electrons from a ^{207}Bi source. With these calibrations we could sum the surface-barrier and plastic-scintillator signals to form a total β energy spectrum which is shown in Fig. 10 along with the shape of an allowed β spectrum. The finite detector energy resolution and scattering of the β's causes the measured spectrum to deviate somewhat from the allowed shape but the qualitative agreement is reasonably good. The surface-barrier signal is also in qualitative agreement with the expected Landau distribution.

The quantities N_+ and N_- (the number of β,γ coincidences when the circular polarimeter preferentially transmitted right and left handed γ's, respectively) were calculated from events in which the γ energy was in the top 15% of the NaI spectrum. After subtracting random coincidences N_+ and N_- were normalized to the same number of decays and dead time corrected. The normalization was done with a scaler which counted the output pulses of a single channel analyzer (SCA) with its window on the photopeak of the 1.778-MeV γ ray. To correct for any difference in the number of decays and any small gain shift in the NaI detector for the two routes, N_+ was multiplied by $(N_{\mathrm{SCA}-})/(N_{\mathrm{SCA}+})$, where $N_{\mathrm{SCA}+(-)}$ is the SCA scaler count for the $+$ $(-)$ route. The dead time correction was done by comparing the total number events recorded in each route of the TAC spectrum to the corresponding number of threefold coincidence gates registered by the fast scalers. Using the corrected N_+ and N_- we obtained $\tilde{A}$ using the relation

$$\tilde{A}=\frac{N_+-N_-}{N_++N_-}\frac{1}{\eta\langle v/c\rangle\langle\cos(\theta)\rangle},$$

where $\langle v/c\rangle$ is the average value of v/c for the betas that pass through the surface barrier detector. This was calculated using the allowed beta shape and the stopping power of the surface-barrier detector. $\langle v/c\rangle=0.948$. $\langle\cos(\theta)\rangle$ is the value of $\cos(\theta)$ averaged over the solid angle of the detector system. $\langle\cos(\theta)\rangle=-0.938$. η is the polarimeter efficiency for a 1.778-MeV γ ray.

$$\eta=0.03090\pm0.00073\ .$$

The asymmetry $\tilde{A}$ was calculated for 19 separate ^{28}Al runs. Combining all runs we obtain

$$\tilde{A}=-0.318\pm0.025\ ,$$

which agrees quite well with the predicted value of $-\frac{1}{3}$. The χ^2 per degree of freedom for these runs was 0.60, which indicates that any fluctuating systematic effects are smaller than the statistical errors.

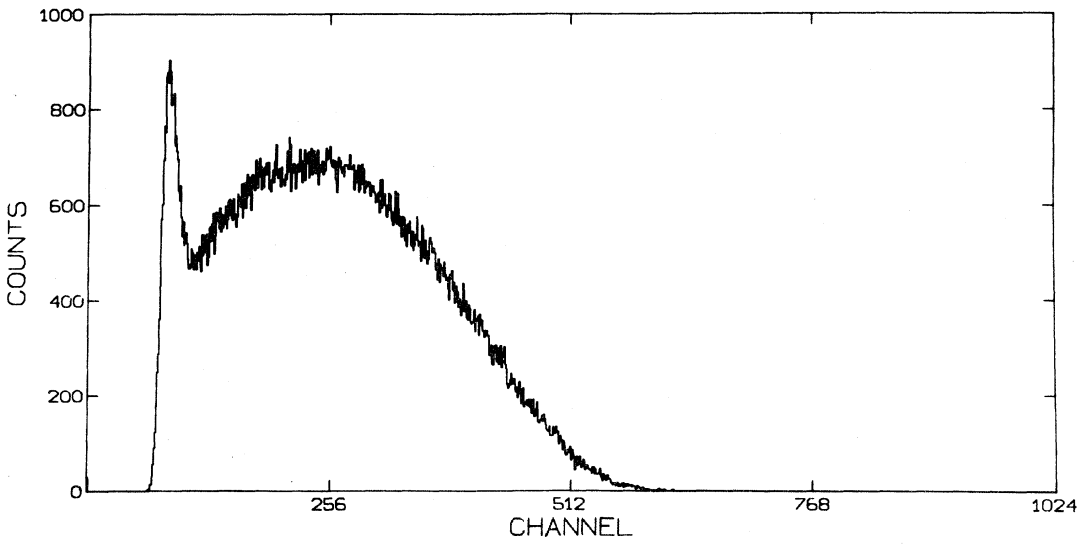

FIG. 11. Plastic scintillator spectrum for ^{27}Si decays. The bump at low energies is due to 511 keV γ rays (see text).

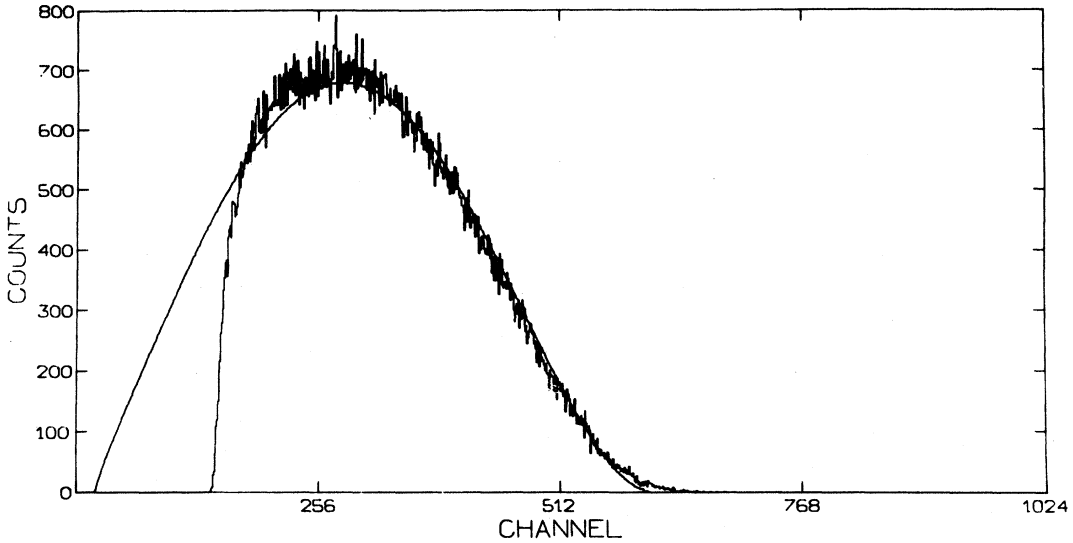

FIG. 12. Total energy spectrum ($E+\Delta E$) for positrons emitted in ^{27}Si decays. The smooth curve is the shape expected in an ideal detector.

B. The β^+ decay of ^{27}Si

The β^+ decay of ^{27}Si was used to check for any differences between the detection of positrons and of electrons. The ^{27}Si β^+ decay (beta end point energy=3.787 MeV) goes to the ground state of ^{27}Al 99.8% of the time. Therefore, no circular polarization measurement was possible, but a comparison of β^+ and β^- spectra could be made.

The ^{27}Si activity was produced via the ^{27}Al$(p,n)^{27}$Si reaction using a 7-MeV proton beam and a 25 μm ^{27}Al foil target. The plastic scintillator and total β^+ energy spectra for plastic scintillator-surface barrier coincidences are shown in Figs. 11 and 12, respectively. The only qualitative difference between the spectra for positrons and electrons is the presence of a feature due to 511-keV γ rays in the positron scintillator spectrum. Such events occur because a positron emitted into the solid angle subtended by the telescope can scatter in the surface

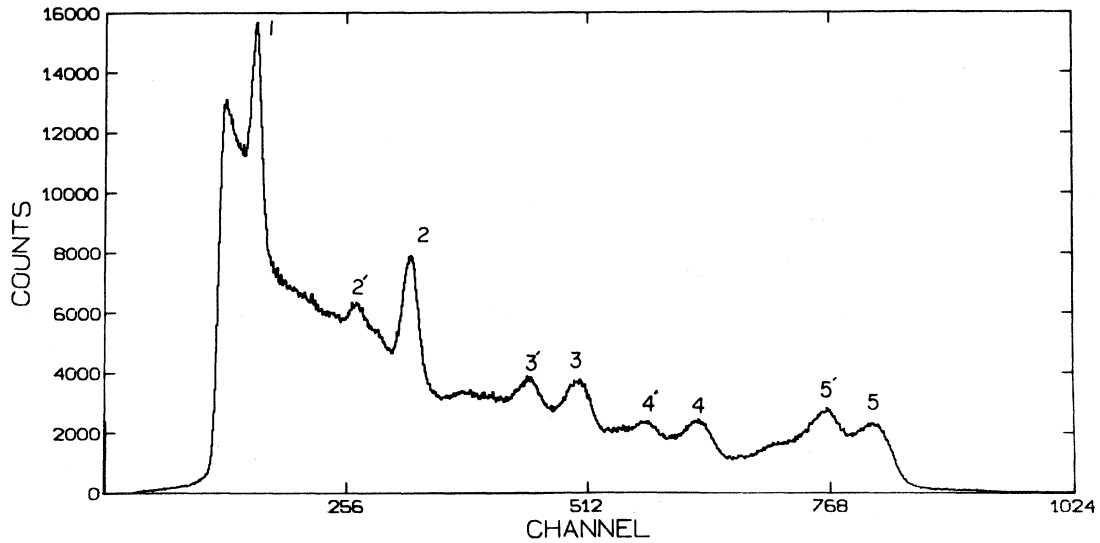

FIG. 13. Spectrum of γ rays from ^{24}Al decay. Peak 1 is the 1.369 MeV γ ray from the 1.369 MeV to ground state transition. Peak 2 (2′) is the photo (first escape) peak for the 2.754 MeV γ ray from the 4.123 to 1.369 MeV transition. Peak 3 (3′) is the photo (first escape) peak for the 4.314 MeV γ ray from the 8.437 to 4.123 MeV transition. Peak 4 (4′) is the photo (first escape) peak for the 5.392 MeV γ ray from the 9.515 to 4.123 MeV transition. Peak 5 (5′) is the photo (first escape) peak for the 7.068 MeV γ ray from the 8.437 to 1.369 MeV transition.

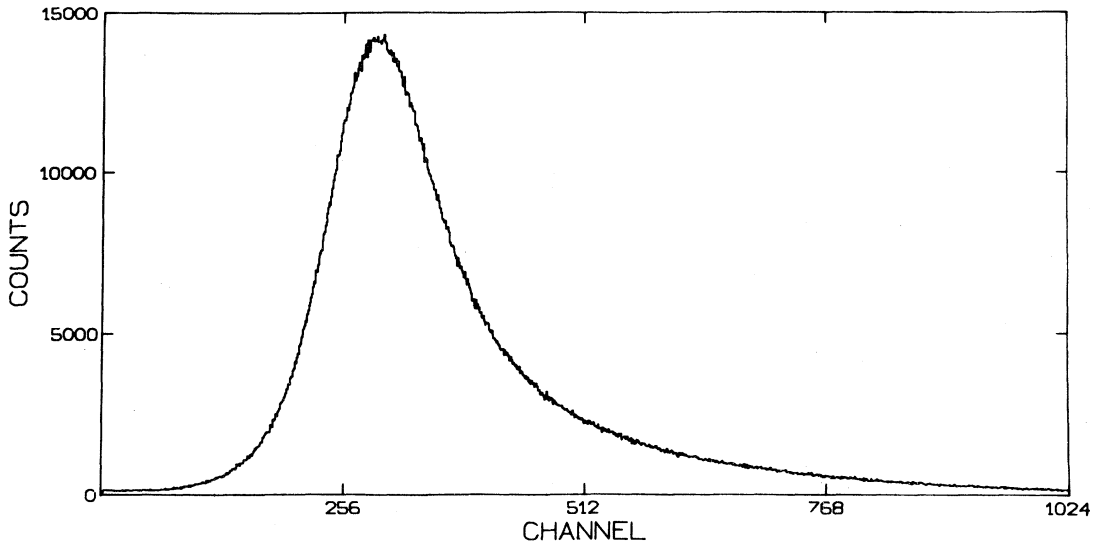

FIG. 14. Spectrum of pulse heights in the surface barrier detector for ^{24}Al decays.

barrier detector, miss the plastic scintillator, annihilate and emit a 511-keV γ ray that is detected by the scintillator. These 511-keV γ rays result from real twofold coincident events, and therefore are expected in all β^+ spectra. The lead shield in the β telescope was designed to minimize the number of such events. The total energy spectrum for the ^{27}Si decay shown in Fig. 12 was generated by including only those plastic signals above the Compton edge of the 511 keV γ rays. The smooth curve is the expected shape for an ideal detector.

C. The β^+ decay of ^{14}O

A zero calibration of the apparatus was done with the β^+ decay of ^{14}O. The ground state of ^{14}O is a 0^+, $T=1$ state that decays 99.4% of the time to the first excited state of ^{14}N which is a 0^+, $T=1$ state that emits a 2.313 MeV γ ray. The $0^+ \rightarrow 0^+$ nature of this decay ensures that the circular polarization asymmetry must be zero.

The ^{14}O was produced via the ^{12}C(^{3}He,n)^{14}O reaction using a 10.5 MeV ^{3}He beam. The 1835 keV end point energy of the ^{14}O decay is so low that most of the β^+ spectrum is below the 511 keV γ ray Compton edge. The SCA window was on the photopeak of the 2313 keV γ ray.

A TAC spectrum for γ rays with energies in the upper 15% of the NaI spectrum was used to calculate N_+ and N_- for each run. The same random background subtraction, normalization, and dead

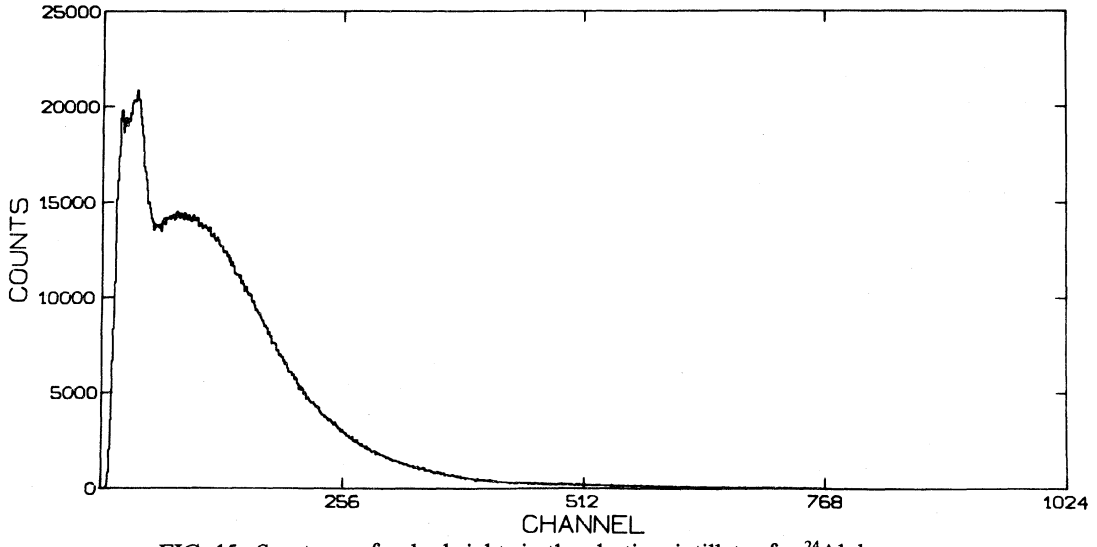

FIG. 15. Spectrum of pulse heights in the plastic scintillator for ^{24}Al decays.

time corrections procedures used in the ^{28}Al analysis were employed. The ^{14}O measurement yields

$$(N_+ - N_-)/(N_+ + N_-) = 0.00175 \pm 0.00262$$

for eight runs with a χ^2 per degree of freedom of 0.70. This agrees well with the expected value of zero.

VI. MEASUREMENT OF THE FERMI MATRIX ELEMENT FOR THE ^{24}Al$\rightarrow^{24}$Mg(8439) TRANSITION

The most intense β^+ branch in ^{24}Al decay is to the 8439 keV 4^+ $T=0$ level of ^{24}Mg (see Fig. 2 and Refs. 11 and 16). Since there is strong evidence that the 8439 and the 9516 4^+ $T=1$ states have very similar spatial structure, we concentrated on measuring the Fermi component of the transition to the 8439 keV level by studying the

$$^{24}\mathrm{Al}(4^+) \xrightarrow{\beta} {}^{24}\mathrm{Mg}(4^+;8439) \xrightarrow{\gamma} {}^{24}\mathrm{Mg}(2^+;1369)$$

$\beta\gamma$ CP correlation. For this correlation we expect $\tilde{A} = (1+y^2)^{-1}\ (-\frac{1}{12} + \sqrt{5/3}\ y)$ where we assume that the $4^+ \rightarrow 2^+$ γ transition is pure $E2$.

The ^{24}Al activity was produced by bombarding 180 μm-thick natural magnesium targets with an 18 MeV proton beam. The ^{24}Al ground state has a half-life of 2.07 sec, while the 439 keV isomer has a half-life of 130 msec. We selected a 7 sec rabbit cycle (3 sec bombardment, 3 sec counting, and 0.5 sec for each transit) so that most of the ^{24}Al^m activity would have decayed during the 0.5 sec transit period (see Ref. 16). Typical NaI, surface barrier, plastic scintillator, and TAC spectra are shown in Figs. 13–16. We are primarily interested in the correlation of β's with the 7.07 MeV γ ray. The Ge(Li) counter spectrum of γ rays following ^{24}Al decay given in Ref. 15 shows that the full energy and first escape peaks of the 7.07 MeV γ ray in our NaI detector do not contain appreciable contamination from other γ-ray lines.

We obtain $\tilde{A}$ for the

$$^{24}\mathrm{Al} \xrightarrow{\beta} {}^{24}\mathrm{Mg}(8439) \xrightarrow{\gamma} {}^{24}\mathrm{Mg}(1369)$$

transition by requiring the β,γ coincidences to satisfy the following conditions:

(1) The NaI pulse height lay within a window embracing the full energy and first escape peaks.

(2) The plastic scintillator signal was above the Compton edge of the 511 keV γ ray.

(3) The TAC signal lay within the real peak.

N^+ and N^- are computed using the same random background subtraction, normalization, and dead time corrections as were employed in the ^{28}Al test case. We extract $\tilde{A}$ from the expression

$$A_{\mathrm{exp}} = \frac{N^+ - N^-}{N^+ + N^-} \frac{1}{\eta \langle v/c \rangle \langle \cos\theta \rangle},$$

where $\langle \cos\theta \rangle = -0.938$, the polarimeter efficiency at $E_\gamma = 7.07$ MeV is $\eta = 0.03054 \pm 0.00072$, and we compute $\langle v/c \rangle = 0.970$ by assuming an allowed shape for the β spectrum and the nominal stopping power of the surface barrier detector. From an analysis of 88 separate data sets we obtain

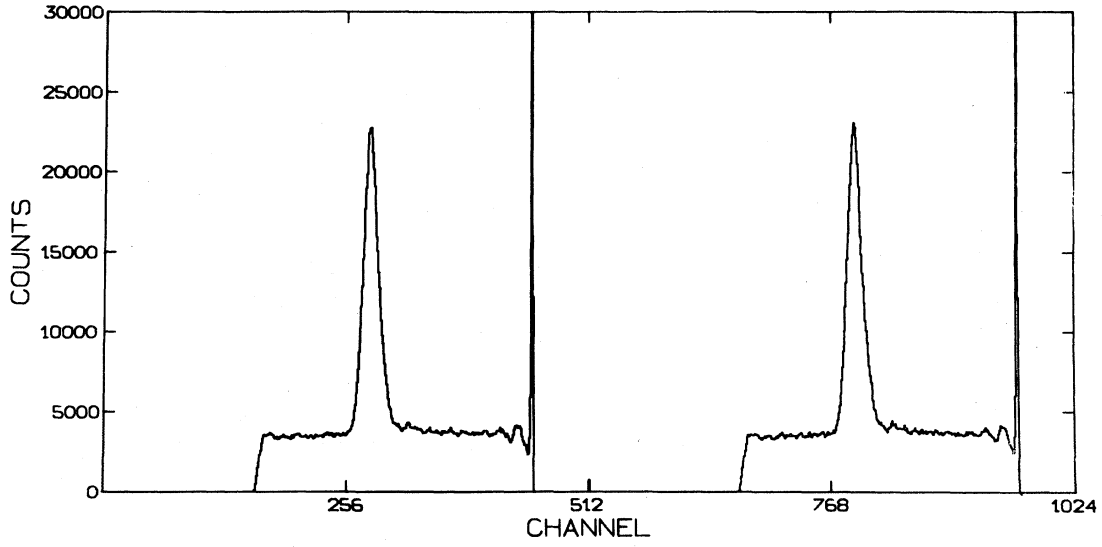

FIG. 16. TAC spectrum for ^{24}Al decays. One channel corresponds to 0.17 nsec.

$\tilde{A}_{\rm exp}=0.145\pm0.030$ with a $\chi^2/\nu=0.91$.

Our measured value $\tilde{A}_{\rm exp}$ cannot be directly compared to a theoretical expression for $\tilde{A}$ for the 8439 keV level because the 8439 keV state is also fed by γ decays of the 9516 keV level. Using the β and γ branching ratios of Ref. 11, we find that for each time the 8439 keV level is directly produced in the β^+ decay of ^{24}Al it is fed $f=0.303\pm0.019$ times by β^+ decay to the 9516 MeV state. Hence the β-γ CP correlation we actually observe $\tilde{A}_{\rm exp}$ is given by

$$W_{8+9}(\theta,\tau)=\frac{1}{1+f}[W_8(\theta,\tau)+fW_9(\theta,\tau)]$$

$$=1+\tilde{A}_{\rm exp}\langle\cos\theta\rangle\langle v/c\rangle\tau\ ,$$

where

$$\tilde{A}_{\rm exp}=\frac{1}{1+f}[\tilde{A}_8+f\tilde{A}_9]$$

and the subscripts 8 and 9 refer to the 8439 and 9516 keV levels, respectively.

We analyze our $\tilde{A}_{\rm exp}$ as follows. Let the unperturbed (good isospin) 8 MeV ($T=0$) and 9 MeV ($T=1$) states be denoted by $|0\rangle$ and $|1\rangle$ with Fermi and GT matrix elements of V, A_0, and A_1, respectively. We assume $V=\sqrt{2}$ and evaluate A_0 and A_1 from the experimental ft values. Now add the effects of a charge dependent interaction $H_{\rm CD}$ with a matrix element $V_{\rm CD}=\langle 1\,|\,H_{\rm CD}\,|\,0\rangle$. This mixes the wave functions to yield

$$|8\rangle=\alpha\,|0\rangle-\beta\,|1\rangle\ ,$$

$$|9\rangle=\alpha\,|1\rangle+\beta\,|0\rangle,\ \ \alpha^2+\beta^2=1\ ,$$

where $V_{\rm CD}=\alpha\beta\Delta E$ with

$$\Delta E=(9516.2-8439.3)\ \text{keV}\ .$$

The Fermi and GT matrix elements of the mixed states become

$$V_8=-\beta V,\ \ A_8=\alpha A_0-\beta A_1\ ,$$

$$y_8=\beta V/(\beta A_1-\alpha A_0),\ \ V_9=\alpha V\ ,$$

$$A_9=\alpha A_1+\beta A_0,\ \ y_9=\alpha V/(\alpha A_1+\beta A_0)\ .$$

From the expressions given earlier, we obtain

$$\tilde{A}_8=\frac{1}{1+{y_8}^2}(C_1+C_2y_8)$$

with $C_1=-\frac{1}{12}$ and $C_2=\sqrt{5}/3$,

$$\tilde{A}_9=\frac{U_1}{1+{y_9}^2}(C_1+C_2y_9)\ \text{and}\ U_1=0.9500\ ,$$

$$ft_8=6250\ \text{sec}/({V_8}^2+{A_8}^2)\ ,$$

$$ft_9=6250\ \text{sec}/({V_9}^2+{A_9}^2)\ ,$$

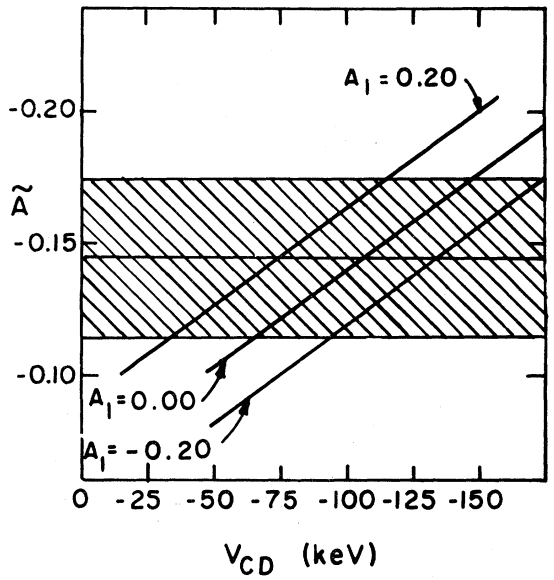

FIG. 17. Predicted values of $\tilde{A}_{\rm exp}$ as a function of $V_{\rm CD}$ (see text). The experimental result of this paper is shown as the shaded band.

where the U_1 coefficient for the unobserved $4^+\rightarrow4^+$ γ ray was evaluated assuming the transition is pure $M1$.

From the experimental values for ft_8 and ft_9 we conclude that $|A_0|$ is quite large, but that $|A_1|$ must be very small. We shall see below that these values are consistent with a simple Nilsson model picture, a simple SU(3) calculation,[11] and with a complete (2*sld*) (Ref. 8) shell model calculation[17] which give 0, 0, and 0.137 for the A_1 matrix element, respectively.

For any value of A_1 we can compute the expected value of $\tilde{A}_{\rm exp}$ as a function of $V_{\rm CD}$ with A_0 always adjusted to fit the experimental value of ft_8. This yields a set of curves for various values of A_1 as shown in Fig. 17. For $A_1=0$ we infer $V_{\rm CD}=-106\pm40$ keV. The sign of $V_{\rm CD}$ is determined by $\tilde{A}_{\rm exp}$ and the assumed sign of A_0. We have taken the sign of A_0 from the Nilsson model calculation discussed below. From the curves for $A_1=+0.20$ and $A_1=-0.20$ we see that the extracted value of $V_{\rm CD}$ is not particularly sensitive to the presence of a small but finite value for A_1. It should be noted that our $A_1=0$ prediction for ft_9 is $\log ft_9=3.498$ which is consistent with the value $\log ft_9=3.510\pm0.018$ quoted in Ref. 11, while the prediction for $A_1=+0.20$ is $\log ft_9=3.481$ which is not consistent with the experimental value. Since A_1 is predicted to vanish by simple calculations and these predictions are consistent with ft_9 we quote the $A_1=0$ value as our result. Should a better value

for A_1 become available the corresponding values of V_{CD} can simply be read off Fig. 17.

VII. DISCUSSION

The observation of large values of V_{CD} is particularly interesting because of the possibility that these large matrix elements could provide unambiguous evidence for small $\Delta T=1$ and $\Delta T=2$ components of the short-range NN interaction which are predicted by meson-exchange theories.[18] Evidence for the $\Delta T=2$ force has been found in low energy NN scattering[18] and in $1p$ shell $\Delta T=2$ isospin multiplet mass splittings.[19] On the other hand there is no clear evidence for the $\Delta T=1$ component although it has been suggested (see, for example, Ref. 20) that such a force could explain the systematic underprediction[21] of $\Delta T=1$ mass splittings by calculations of the direct electromagnetic effects. Hence it is interesting to see if the large $\Delta T=1$ matrix elements observed in certain self-conjugate nuclei can be explained by Coulomb forces alone.

We begin by considering the isospin mixing in ^{24}Mg of the lowest 4^+, $T=1$ state, for which we have measured $|V_{CD}|=106\pm40$ keV, and the lowest 1^+, $T=1$ state, for which $|V_{CD}|=49\pm5$ keV has been inferred.[16] This, of course, requires a model of the nuclear states. Previous work (see, for example, Refs. 11 and 22) has shown that the nuclei around $A=24$ are strongly deformed and well described in terms of the Nilsson model.[23] In this model the lowest-lying orbital around the ^{16}O core is number 6 with $|\Omega|=\frac{1}{2}$, followed in order of increasing energy by number 7 with $|\Omega|=\frac{3}{2}$, number 9 with $|\Omega|=\frac{1}{2}$, and number 5 with $|\Omega|=\frac{5}{2}$. The $K=0$ ^{24}Mg ground state band has filled the orbits numbered 6 and 7. The lowest 4^+ state at 4.123 MeV belongs to this $K=0$ band. Low-lying "particle-hole" excitations occur by exciting nucleus from orbit number 7 into orbit numbers 5 or 9. The 4^+ state at 6.010 MeV belongs to a $K=2$ band formed from the orbits numbered 9 and 7, while the 4^+ state at 9.301 MeV belongs to a 2p-2h $K=0$ band. The 4^+, $T=1$ state at 9.516 MeV and the 4^+, $T=0$ state at 8.439 MeV are analog and antianalog $K=4$ states formed by promoting a nucleon from orbit number 7 ($|\Omega|=\frac{3}{2}$) to orbit number 5 ($|\Omega|=\frac{5}{2}$). This same excitation can also couple to $K=1$. The $T=1$ state with this configuration is the 9.966 MeV 1^+ level. The antianalog $T=0$ strength is probably split between the 1^+, $T=0$ states at 7.747 and 9.827 MeV. This simple Nilsson model picture is quite consistent with the β decays of ^{24}Al and ^{24}Al^m. It explains the strong GT decay of ^{24}Al to the 8.439 MeV antianalog state. In the asymptotic limit of the Nilsson model $M_{GT}=-(\frac{8}{5})^{1/2}$ which implies $\log ft=3.39$ if we use free-nucleon GT moments. This compares reasonably well to the measured value[11] of 3.93 ± 0.02 since we have ignored any quenching of the GT moments. The model accounts for the very small GT contribution to the decay of ^{24}Al to the 9.516 MeV analog state[16] as well. In the asymptotic limit $M_{GT}=0$, which, assuming that $M_F=\sqrt{2}$, implies $\log ft=3.49$. This agrees with the measured value[11] of 3.510 ± 0.018. The model also accounts for the ratio of β decay strengths to the 10.576 MeV (5^+, $K=4$) and 8.439 MeV (4^+, $K=4$) states. Although the decays of ^{24}Al^m (1^+) are not as well studied the model gives a qualitative explanation for these results (see Ref. 16) as well. In this case the asymptotic Nilsson model predicts a vanishing M_{GT} for the antianalog transition and a large M_{GT} for the analog decay, which is consistent with the results[16] if one includes isospin mixing.

Now we consider the isospin mixing matrix elements connecting $T=1$ analog and $T=0$ antianalog states—following closely simple arguments presented in more detail in Ref. 10. If the charge-dependent interaction, H_{CD}, is the Coulomb force (or, more generally, obeys, in the notation of Ref. 18, the symmetries $V_{II}=V_{III}$ and $V_{IV}=0$) then $\langle T=0|H_{CD}|T=1\rangle$ can be expressed in terms of differences of isovector single-particle energy $C(i)$ and $C(j)$ and differences of isovector two-body interactions $C(ii)$ and $C(ij)$, where i and j refer to the active Nilsson orbitals. In particular, one finds that

$$\langle T=1|H_{CD}|T=0\rangle = \tfrac{1}{2}[C(j)-C(i)+C(ij)-C(ii)] .$$

If one assumes that the C coefficients vary negligibly as one changes A by ±1 and have negligible dependence on excitation energy, then our simple model allows us to determine the C coefficients from the measured mass splittings in the $T=1$ multiplet in mass A and the $T=\frac{1}{2}$ multiplets in masses $A-1$ and $A+1$. For example, using the simple wave functions shown schematically in Fig. 18, we obtain the relations

$$\begin{aligned}\langle 4^+\ K=4,T=1|H_{CD}|4^+\ K=4,T=0\rangle &= \tfrac{1}{2}[(^{25}\mathrm{Al}-{}^{25}\mathrm{Mg})-(^{23}\mathrm{Mg}-{}^{23}\mathrm{Na}) \\ &\quad -(^{24}\mathrm{Al}-2{*}{}^{24}\mathrm{Mg}{*}+{}^{24}\mathrm{Na})] \\ &= \sim 71\ \mathrm{keV} ,\end{aligned}$$

where ^{25}Al, ^{25}Mg, ^{23}Mg, ^{24}Al, and ^{24}Na refer to ground state masses and ^{24}Mg* to the mass of the 4^+, $T=1$ analog state. The "prediction" of our simple model is consistent with our measurement of -106 ± 40 keV. On the other hand the simple

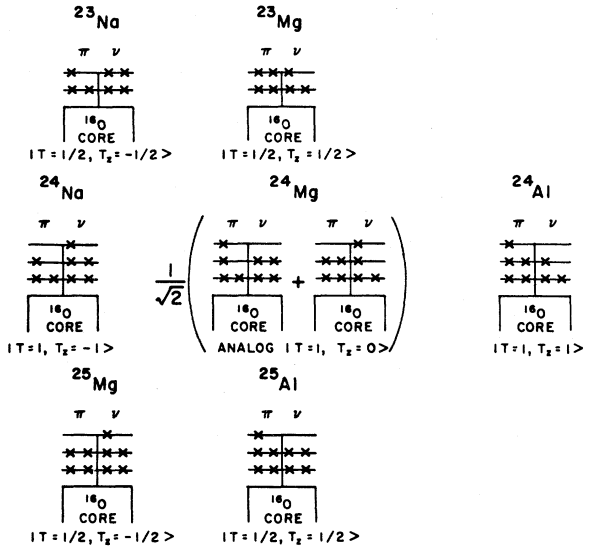

FIG. 18. Schematic Nilsson wave functions used to relate analog antianalog mixing to mass differences. In order of increasing energy the orbits are numbers 6, 7, and 5.

model predicts that

$$\langle 4^+, K=4, T=1 \,|\, H_{\mathrm{CD}} \,|\, 4^+, K=0, T=0\rangle = 0$$

since the matrix element is four times K forbidden. This is qualitatively consistent with the observed value[1] of 5.4±2.2 keV. By applying these same arguments[10] to the 1^+ states we predict that

$$\langle 1^+, K=1, T=1 \,|\, H_{\mathrm{CD}} \,|\, 1^+, K=1, T=0\rangle = -76 \text{ keV} .$$

This is larger than the observed value[16] of $|\langle H_{\mathrm{CD}}\rangle| = 49\pm5$ keV for the matrix element connecting the 1^+, $T=1$ state with the 9.827 MeV state. However, as was noted above and in Refs. 11 and 16, a significant fraction of the 1^+ antianalog strength is located in the 7.747 MeV state. Thus one expects the model to overestimate the matrix element connecting the 1^+, $T=1$ state to the 9.827 MeV level.

The success of our highly simplified model for predicting $\langle H_{\mathrm{CD}}\rangle$ for analog antianalog mixing leads us to apply the results to similar cases in $A=8$ (Refs. 5 and 6), $A=12$ (Refs. 7 and 8), and $A=16$ (Ref. 9). The predicted and measured matrix elements are shown in Table II. Considering the crudeness of our approximation, particularly the assumption that the charge-dependent single-particle energies are independent of excitation energy and small changes in mass number, the agreement is quite impressive. The agreement is poorest in $A=8$, which is precisely where one expects these approximations to be most artificial.

TABLE II. Measured isospin mixing matrix elements compared to schematic model predictions.

Nucleus	Levels	$\langle V_{\mathrm{CD}}\rangle_{\mathrm{exp}}$[a]	$\langle V_{\mathrm{CD}}\rangle_{\mathrm{th}}$[b]
^{8}Be (2^+)	16.6 16.9	−145 keV	−88 keV[c]
^{12}C (1^+)	12.7 15.1	−130±26 keV	−125 keV
^{16}O (2^-)	12.5 13.0	≤ −155±30 keV	−163 keV
^{24}Mg (4^+)	8.4 9.5	−106±40	−71 keV

[a]See text for references.
[b]Computed using model of Ref. 10 as discussed in text.
[c]In this case the T mixing is so large that we used the unperturbed mass of ^{8}Be* in the schematic model prediction.

One could (and we do) interpret this agreement as follows. Since our model, which assumes Coulomb-like forces, is fairly successful there is no clear evidence for non-Coulomb (i.e., short-range) charge dependent forces from the isospin mixing data. On the other hand we know from other sources (see, for example, Ref. 19) that a $\Delta T=2$ short-range V_{II} interaction having the same *sign* as the Coulomb force is present. If a $\Delta T=1$ short-range interaction, also having the *sign* of the Coulomb force, were present it would tend to preserve the Coulomb symmetry of V_{II}-V_{III} and therefore not violate our simple relations. Note that a V_{III} of this sign would tend to "explain" the Nolen-Schiffer anomaly.

VIII. CONCLUSIONS

We have used rigorous methods to observe the largest isospin mixing matrix element ever detected in β decay. This matrix element (−106±40 keV) arises from the mixing of analog and antianalog $K=4$ levels. It is much larger than the previously measured matrix element of 5.4±2.2 keV connecting the $K=4$ 4^+, $T=1$ level with the $K=0$ 4^+, $T=0$ level. This clearly demonstrates the importance of analog-antianalog mixing in isospin impurities. We can account for this matrix element by using a simple model which assumes that the only charge dependent interaction is the Coulomb force. From the success of this simple model we draw the conclusion that it will be very difficult to learn about (small) short-range charge-dependent forces from isospin admixtures. Future work aimed at studying such forces should probably concentrate on small effects in multiplet mass splittings since the mass data are inherently more precise than isospin mixing results.

ACKNOWLEDGMENTS

We thank Prof. A. B. McDonald for the loan of two circular polarimeters and Dr. B. A. Brown for informative discussions. E.G.A. is grateful for a J. S. Guggenheim Fellowship and an A.v. Humboldt Prize which permitted this paper to be written during very pleasant visits to Oxford and Heidelberg. This work was supported in part by the U.S. Department of Energy.

---

*Present address: Shell Oil, Rocky Mountain Division, Houston, TX 77002.
†Deceased.
‡Present address: Physics Department, Temple University, Philadelphia, PA 19104.

[1]S. Raman, T. A. Walkiewicz, and H. Behrens, At. Data Nucl. Data Tables 16, 451 (1975).
[2]P. A. Dickey, J. E. Bussoletti, and E. G. Adelberger, Nucl. Phys. A303, 442 (1978).
[3]D. E. Alburger and E. K. Warburton, Phys. Rev. C 20, 793 (1979).
[4]D. M. Perlman, L. Grodzins, and C. E. Thorn, Phys. Rev. C 18, 2333 (1978).
[5]P. Paul, D. Kohler, and K. A. Snover, Phys. Rev. 173, 919 (1968).
[6]C. P. Browne, W. D. Callender, and J. R. Erskine, Phys. Lett. 23, 371 (1966).
[7]J. B. Flanz, R. S. Hicks, R. A. Lindgren, G. A. Peterson, J. Dubach, and W. C. Haxton, Phys. Rev. Lett. 43, 1922 (1979).
[8]E. G. Adelberger, R. E. Marrs, K. A. Snover, and J. E. Bussoletti, Phys. Rev. C 15, 484 (1977).
[9]G. J. Wagner, K. T. Knöpfle, G. Mairle, P. Doll, H. Hafner, and J. L. C. Ford, Jr., Phys. Rev. C 16, 1271 (1977).
[10]A. B. McDonald and E. G. Adelberger, Phys. Rev. Lett. 40, 1692 (1978).
[11]E. K. Warburton, C. J. Lister, D. E. Alburger, and J. W. Olness, Phys. Rev. C 23, 1242 (1981).
[12]H. Behrens and J. Jänecke, *Landolt-Börnstein: Numerical Tables for Beta Decay and Electron Capture* (Springer, Berlin, 1969), New Series, Group 1, Vol. 4.
[13]R. M. Steffen and K. Alder in *The Electromagnetic Interaction in Nuclear Spectroscopy,* edited by W. D. Hamilton (North-Holland, Amsterdam, 1975), p. 505.
[14]E. D. Earle, A. B. McDonald, E. G. Adelberger, K. A. Snover, H. E. Swanson, R. Von Lintig, H. B. Mak, and C. A. Barnes, Proceedings of the International Conference on Nuclear Structure, Amsterdam, 1982 (unpublished).
[15]R. B. Chesler, Nucl. Instrum. Methods 37, 185 (1965).
[16]A. Ray, C. D. Hoyle, and E. G. Adelberger, Nucl. Phys. A378, 29 (1982).
[17]B. A. Brown, W. Chung, and B. H. Wildenthal (unpublished); Phys. Rev. Lett. 40, 1631 (1978).
[18]E. M. Henley and G. A. Miller in *Mesons in Nuclei,* edited by M. Rho and D. Wilkinson (North-Holland, Amsterdam, 1979), p. 406.
[19]R. D. Lawson, Phys. Rev. C 19, 2359 (1979).
[20]S. Shlomo and D. O. Riska, Nucl. Phys. A254, 281 (1975).
[21]J. A. Nolen, Jr. and J. P. Schiffer, Annu. Rev. Nucl. Sci. 19, 471 (1969).
[22]J. D. Garrett, H. T. Fortune, R. Middleton, and W. Scholz, Phys. Rev. C 18, 2032 (1978).
[23]S. Nilsson, K. Dan. Vidensk. Selsk. Mat.-Fys. Medd. 29, No. 16 (1955).